Phytochemistry 100 (2014) 141–149

Contents lists available at ScienceDirect

Phytochemistry

journal homepage: www.elsevier.com/locate/phytochem

Balsacones D-I, dihydrocinnamoyl flavans from *Populus balsamifera* buds

François Simard, Jean Legault, Serge Lavoie, André Pichette *

Laboratoire d'Analyse et de Séparation des Essences Végétales (LASEVE), Département des sciences fondamentales, Université du Québec à Chicoutimi, Québec G7H 2B1, Canada

ARTICLE INFO

Article history:
Received 23 May 2013
Received in revised form 25 November 2013
Available online 30 January 2014

Keywords:
Populus balsamifera L.
Salicaceae
Bud
Flavan
Dihydrochalcone
Balsacone
Chiral separation
Circular dichroism
Antibacterial activity
Staphylococcus aureus
Computational calculations

ABSTRACT

A phytochemical investigation of an ethanolic extract from *Populus balsamifera* L. buds resulted in the isolation and characterization of twelve new flavan derivatives consisting of six pairs of enantiomers. Structures of (+) and (−)-balsacones D-I were elucidated based on spectroscopic data (1D and 2D NMR, MS) and their absolute configurations were established using X-ray single crystal diffraction analysis and ECD computational calculations. Antibacterial activity and cytotoxicity of all purified enantiomers were evaluated *in vitro* against *Staphylococcus aureus* and human skin fibroblast cells, respectively.

Introduction

The genus *Populus* includes nearly 30 species distributed mostly throughout the northern hemisphere (Dickmann, 2001). Buds from several *Populus* species are covered with an exudate (Eckenwalder, 1996; Greenaway and Whatley, 1990) that has attracted growing interest in the scientific community since it has been identified as a known plant source of propolis (Bankova et al., 2002; Salatino et al., 2011). Propolis is a bee product that has been used in folk medicines around the world for the treatment of wounds and burns, sore throat, stomach ulcers, etc. (Bankova, 2005; Salatino et al., 2011). Several studies about propolis have established similarities between the compositions of poplars buds exudate (PBE) and what is sometimes referred to as poplar-type propolis. For example, hydroxycinnamates and their derivatives, which are characteristic constituents of PBE from the entire genus *Populus* (Chen et al., 2009; Tsai et al., 2006), have been identified many times in propolis (Salatino et al., 2011). Other species-specific components of *Populus*, such as dihydrochalcones present in PBE from section *Tacamahaca*, have also been described in propolis (Christov et al., 2006). On the other hand, only a handful of studies about biological and pharmacological properties of PBE are available. Vardar-Ünlü et al. demonstrated that bud extracts from different *Populus* species possess antibacterial activity similar to that of poplar-type propolis (Vardar-Ünlü et al., 2008). Antioxidant properties were also detected for *Populus nigra* bud extract (Dudonné et al., 2011). Close relations between the chemical compositions of poplar type propolis and PBE suggest that PBE might be an interesting untapped source for the discovery of new bioactive compounds.

The exudate covering buds from *Populus balsamifera* L. (section *Tacamahaca*) has a strong balsam smell in the spring. Amongst others, North American aboriginals used tincture or poultice of *P. balsamifera* buds as dermatological and gastrointestinal aids as well as for the treatment of chronic rheumatism (Moermann, 1998). Earlier studies established that buds are rich in phenolic compounds, such as simple phenols and phenolic acids (Isidorov and Vinogorova, 2003; Mattes et al., 1987; Pearl and Darling, 1968b; Reichardt et al., 1990; Sentsov et al., 1997), phenolic glycosides (Pearl and Darling, 1968b), hydroxycinnamic acids and their esters (Greenaway et al., 1992a,b; Greenaway and Whatley, 1990; Isidorov and Vinogorova, 2003; Pearl and Darling, 1968a), flavones and flavanones (Isidorov and Vinogorova, 2003; Kurkin et al., 1990; Sentsov et al., 1997), chalcones and dihydrochalcones (Greenaway et al., 1992a, 1989; Greenaway and Whatley, 1990; Kurkin et al., 1990). However, little work has been conducted on their biological and pharmacological potential. Recently, the LASEVE team identified three new hydroxycinnamylated dihydrochalcones from an ethanolic extract of *P. balsamifera* buds (Lavoie et al., 2013). Balsacone A, B and C, were found active against *Staphylococcus aureus*

* Corresponding author. Tel.: +1 418 545 5011; fax: +1 418 545 5012.
E-mail address: andre_pichette@uqac.ca (A. Pichette).

0031-9422/$ - see front matter Crown Copyright © 2014 Published by Elsevier Ltd. All rights reserved.
http://dx.doi.org/10.1016/j.phytochem.2013.12.018

with MIC values ranging from 3.1 to 6.3 μM. Continuing the search for new antibacterial compounds, the ethanol extract of buds from *P. balsamifera* has been further investigated. The isolation and structural elucidation of 12 new flavan derivatives which have been isolated as 6 pairs of enantiomers is reported in the present paper. The antibacterial activity and the cytotoxicity of these compounds were also evaluated against *S. aureus* and human skin fibroblast cells respectively.

Results and discussion

Structural determination

Fractionation of *P. baslamifera* bud ethanolic extract by liquid–liquid extraction, silica gel column chromatography and reversed phase flash chromatograhy followed by semi-preparative HPLC purification yielded compounds **1–6** (Fig. 1).

Balsacone D (**1**) was isolated as a yellow powder and its molecular formula was established as $C_{24}H_{22}O_5$ based on the $[M+Na]^+$ quasimolecular ion peak at *m/z* 413.1374 in the HRMS spectrum. The IR spectrum showed bands at 3347 and 1615 cm^{-1}, due to phenol and carbonyl functions, respectively. The ^{13}C and DEPT-135 NMR spectra afforded signals accounting for 20 carbons, i.e. one carbonyl, four oxygenated quaternary aromatic carbons, six sp^2 and one oxygenated sp^3 methines, four aromatic quaternaries and four methylenes. Detail analysis of 1D ^1H, 2D-COSY and HSQC experiments (Fig. 2) showed resonances for a 1,4 disubstituted aromatic ring at δ_H 7.35 (2H, d, *J* = 8.5 Hz, H-2′/H-6′) and 6.85 (2H, d, *J* = 8.5 Hz, H-3′/H-5′) and a mono-substituted aromatic ring at δ_H 6.91 (2H, d, *J* = 7.3 Hz, H-2″/H-6″), 7.16 (2H, t, *J* = 7.3 Hz, H-3″/H-5″) and 7.10 (1H, t, *J* = 7.3 Hz, H-4″). Two other spin systems could be observed in the COSY, i.e. two methylenes

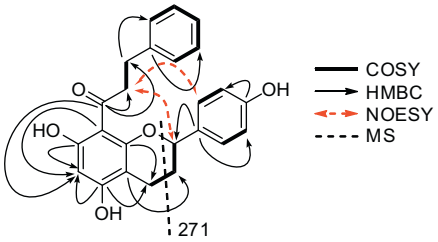

Fig. 2. HMBC, COSY, NOESY and MS key data for identification of compound **1**.

at δ_H 2.84 (2H, t, *J* = 8.1 Hz, H-7″) and 3.24 (2H, m, H-8″) and a AA′BB′M system at δ_H 2.06 (1H, m, H-3a), 2.19 (1H, m, H-3b), 2.68 (1H, m, H-4a), 2.78 (1H, ddd, *J* = 17.0, 5.9, 2.4 Hz, H-4b) and 5.07 (1H, dd, *J* = 11.0, 2.0 Hz, H-2). Also, the presence of a chelated hydroxyl proton was detected based on the signal at δ_H 13.82 (1H, s, 7-OH) on the 1D ^1H spectrum. The HMBC correlations of δ_C 205.2 (C-9″) with H-7″ and H-8″ and of δ_C 31.2 (C-7″) with H-2″/H-6″ suggested that the two methylenes were linked to a ketone and to the monosubstituted aromatic ring resulting in a dihydrocinnamoyl moiety. The HMBC correlations of δ_C 158.3 (C-4′) with H-3′/H-5′ and of δ_C 132.7 (C-1′) with H-2′/H-6′ and H-2 indicated that the 1,4 disubstituted aromatic ring was hydroxylated and branched to the AA′BB′M system. The six remaining carbon resonances at δ_C 163.2 (C-5), 96.1 (C-6), 166.0 (C-7), 105.7 (C-8), 159.7 (C-9) and 102.0 (C-10) were assigned to a third aromatic ring. This third aromatic ring was also attached to the AA′BB′M spin system as shown by the HMBC correlation of C-5 with H-4a and H-4b which suggested it might be forming the ring A of a flavan skeleton hydroxylated in position 5, 7 and 4′. The proton signal at δ_H 6.02 (1H, s, H-6) implied the presence of a pentasubstituted ring A to

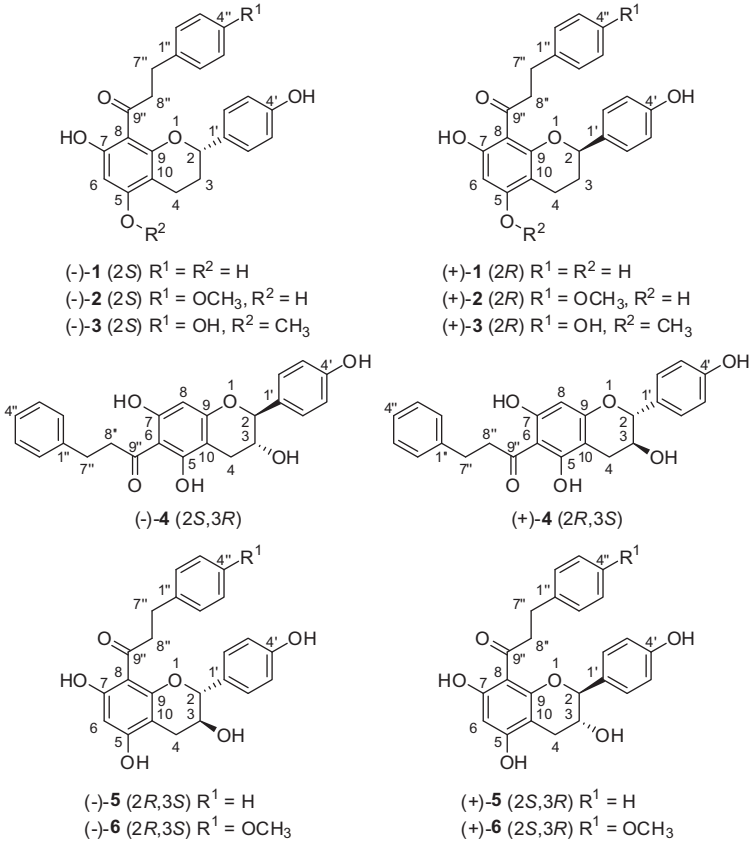

Fig. 1. Structures of **1–6.**

which the dihydrocinnamoyl unit would be attached. The presence of a peak at *m/z* 271 on the mass spectrum (APCI) representing the fragment obtained by the typical retro Diels–Alder fragmentation reaction of flavonoids (Pelter et al., 1965) confirmed the attachment of the dihydrocinnamoyl moiety to the A ring. A W-coupling between C-9″ and H-6 was also present in the HMBC spectrum. From these observations, only two possibilities can be considered for the position of the dihydrocinnamoyl moiety, i.e. C-6 and C-8. The 2D-NOESY correlations of H-8″ with H-2 and H-2′/H-6′ confirmed that the dihydrocinnamoyl moiety was attached at C-8 and therefore the resonance at δ_H 6.02 could be assigned to H-6. Assignments of positions 5, 7, and 9 were determined using HMBC correlations of C-5 and C-7 with H-6 and of C-5 and C-9 with H-4a and H-4b. The signal at δ_C 102.0 was assigned as C-10 based on its HMBC correlations with H-3b and therefore, the resonance at δ_C 105.7 was assigned as C-8, the only remaining position. Based on the above evidence, balsacone D (**1**) was characterized as 8-(dihydrocinnamoyl)-5,7,4′-trihydroxyflavan.

Balsacone E (**2**) was isolated as a yellow powder and its molecular formula was established as $C_{25}H_{24}O_6$ based on the $[M+H]^+$ quasimolecular ion peak at *m/z* 421.1656 in the HRMS spectrum. The IR spectrum had bands at 3400 and 1622 cm^{-1}, due to phenol and carbonyl functions, respectively. The ^1H and ^{13}C NMR spectra showed the presence of the same 5,7,4′-trihydroxyflavan skeleton as for compound **1** but with a different substituent at C-8. Analysis of 1D ^1H, 2D-COSY and HSQC experiments showed signals for a 1,4 disubstituted aromatic ring at δ_H 6.79 (2H, d, *J* = 8.7 Hz, H-2″/H-6″) and 6.72 (2H, d, *J* = 8.7 Hz, H-3″/H-5″) and two methylenes at 2.77 (2H, m, H-7″) and 3.19 (2H, m, H-8″). The HMBC correlations of δ_C 205.4 (C-9″) with H-7″ and H-8″ and of δ_C 30.3 (C-7″) with H-2″/H-6″ suggested that the two methylenes were linked to a ketone and to the 1,4-disubstituted aromatic ring. The HMBC correlations of δ_C 158.7 (C-4″) with H-3″/H-5″ and δ_H 3.74 (4″-O-CH_3) established that the 1,4-disubstituted aromatic ring was methoxylated. It was, therefore, concluded that the C-8 substituent was a 4-methoxydihydrocinnamoyl moiety. The 2D NOESY correlations of H-8″ with δ_H 5.08 (1H, dd, *J* = 10.7, 2.3 Hz, H-2) and 7.37 (1H, d, *J* = 8.5 Hz, H-2′/H-6′) confirmed that the 4-methoxydihydrocinnamoyl moiety was in C-8. From the above evidence, balsacone E (**2**) was characterized as 8-(4-methoxydihydrocinnamoyl)-5,7,4′-trihydroxyflavan.

Balsacone F (**3**) was isolated as a yellow powder and its molecular formula was established as $C_{25}H_{24}O_6$ based on the $[M+Na]^+$ quasimolecular ion peak at *m/z* 443.1477 in the HRMS spectrum. The IR spectrum showed bands at 3363 and 1617 cm^{-1}, due to phenol and carbonyl functions, respectively. The ^1H and ^{13}C NMR spectroscopic data were closely related to **2** suggesting that **3** was an isomer. Indeed, after detailed analysis of NMR spectra, the only difference accounted for was the position of the methoxy group, which was determined as C-5 by the HMBC correlation of δ_C 164.7 (C-5) with δ_H 3.89 (3H, s, OCH_3). Based on the above evidence, balsacone F (**3**) was characterized as 8-(4-hydroxydihydrocinnamoyl)-7,4′-dihydroxy-5-methoxyflavan.

Balsacone G (**4**) was obtained as a yellow powder and its molecular formula was established as $C_{24}H_{22}O_6$ based on the $[M+Na]^+$ quasimolecular ion peak at *m/z* 429.1330 in the HRMS spectrum. The IR spectrum had bands at 3300 and 1628 cm^{-1}, due to phenol and carbonyl functions, respectively. Details analysis of 1D ^1H, 2D-COSY, HSQC and HMBC showed the presence of a 3,5,7,4′-tetrahydroxyflavan skeleton and a dihydrocinnamoyl moeity. HMBC correlations of δ_C 161.8 (C-9) with δ_H 4.80 (1H, d, *J* = 7.5 Hz, H-2) and 5.97 (1H, s, H-8) indicated that position C-8 on the 3,5,7,4′-tetrahydroxyflavan skeleton is protonated. Also, a W-coupling between δ_C 205.6 (C-9″) and H-8 was observed on the HMBC spectrum indicating that the dihydrocinnamoyl unit was attached at C-6. Based on the above evidence, balsacone G (**4**) was characterized as 6-(dihydrocinnamoyl)-3,5,7,4′-tetrahydroxyflavan.

Balsacone H (**5**) was obtained as a yellow powder and its molecular formula was established as $C_{24}H_{22}O_6$ based on the $[M+K]^+$ quasimolecular ion peak at *m/z* 445.1055 in the HRMS spectrum. The IR spectrum showed bands at 3450 and 1632 cm^{-1}, due to phenol and carbonyl functions, respectively. Details analysis of the 1D ^1H, 2D-COSY and HSQC showed the presence of the same 3,5,7,4′-tetrahydroxyflavan skeleton and dihydrocinnamoyl unit as in **4**. However, the ^1H NMR and ^{13}C spectra of **5** shows discrepancies from those of **4**. These discrepancies were attributed to the position of attachment of the dihydrocinnamoyl unit which was proposed to be C-8 instead of C-6. The C-8 attachment was confirmed by the HMBC correlations of δ_C 158.7 (C-9) with δ_H 4.81 (1H, d, *J* = 8.4 Hz, H-2) and of δ_C 163.3 (C-5) and 166.1 (C-7) with δ_H 6.05 (1H, s, H-6). Based on the above evidence, balsacone H (**5**) was characterized as 8-(dihydrocinnamoyl)-3,5,7,4′-tetrahydroxyflavan.

Balsacone I (**6**) was obtained as a yellow powder and its molecular formula was established as $C_{25}H_{24}O_7$ based on the $[M+Na]^+$ quasimolecular ion peak at *m/z* 459.1431 in the HRMS spectrum. The IR spectrum showed bands at 3337 and 1614 cm^{-1}, due to phenol and carbonyl functions, respectively. The ^1H and ^{13}C NMR spectra were almost identical to those of compound **5,** but with an additional methoxy group at δ_H 3.74 (3H, s, OCH_3) and δ_C 55.3 (OCH_3). This group was assigned at 4″ from the HMBC correlation between δ_C 158.7 (C-4″) and the methoxy protons. 2D-NOESY correlations of δ_H 7.36 (2H, d, *J* = 8.6 Hz, H-2′/H-6′) with 2.76 (2H, t, *J* = 7.9 Hz, H-7″) and δ_H 3.16 (2H, m, H-8″) further confirmed that the (4-methoxydihydrocinnamoyl moiety was located at C-8. Based on the above evidence, balsacone I (**6**) was characterized as 8-(4-methoxydihydrocinnamoyl)-3,5,7,4′-tetrahydroxyflavan.

Measurement of the optical rotation of compounds **1**–**6** yielded $[\alpha]_d$ values of 0. Furthermore, no Cotton Effect (CE) was observed on their ECD spectra suggesting that they were racemic. Chiral analytical HPLC confirmed the presence of two compounds in equal amounts (Fig. S-25 to S-30) and chiral semi-preparative HPLC purification yielded the (+) and (−) enantiomers for the six racemic mixtures (**1**–**6**). Crystals of (−)-**1** were obtained after drying an (isopropyl alcohol) IPA solution under a N_2 stream. Single-crystal X-ray diffraction analysis allowed us to determine that the C-2 absolute configuration of (−)-**1** was *S* (Fig. 3). The absolute configuration of other purified enantiomers was determined by comparing their experimental ECD spectra with the calculated ones obtained using the time dependent density functional theory (TDDFT) method (Fig. 4). Comparison of the experimental ECD spectrum of (−)-**1** with calculated ECD spectrum of (2*S*)-**1** (Fig. 4) further confirmed its 2*S* absolute configuration. Indeed, the calculated ECD spectrum showed a positive CE at 214 nm and two negative CEs at 238 and 271 nm which were in good agreement with the experimental spectrum (Fig. 4). It is interesting to note that X-ray diffraction analysis (Fig. 3) and conformational calculations (Fig. S-31) both showed that the pyran ring of (−)-**1** had a half-chair conformation with *P*-helicity. The negative ^1L_b band CE (288 nm) observed on the experimental ECD spectrum of (−)-**1** was, therefore, consistent with the helicity rule established for the chroman chromophore (Kurtán et al., 2012; Slade et al., 2005). The experimental ECD spectrum of (+)-**1** showed CEs of opposite signs, i.e. one negative at 227 nm and two positive at 239 and 288 nm, thus confirming its 2*R* absolute configuration. In the case of (−)-**2** and (−)-**3,** the positive CE at 224 nm and the two negative CEs at 239 and 289 nm, observed on their experimental ECD spectrum, correlated well with the calculated ECD spectra of 2*S*-**2** and 2*S*-**3**, respectively (Fig. 4). The absolute configurations of (+)-**2** and (+)-**3** were determined to be 2*R* based on the negative and the two positive CEs observed on both ECD spectrum at 224, 239 and 289 nm, respectively. For compound **4**, a relative trans 2,3 configuration with the hydroxyphenyl and the hydroxyl in

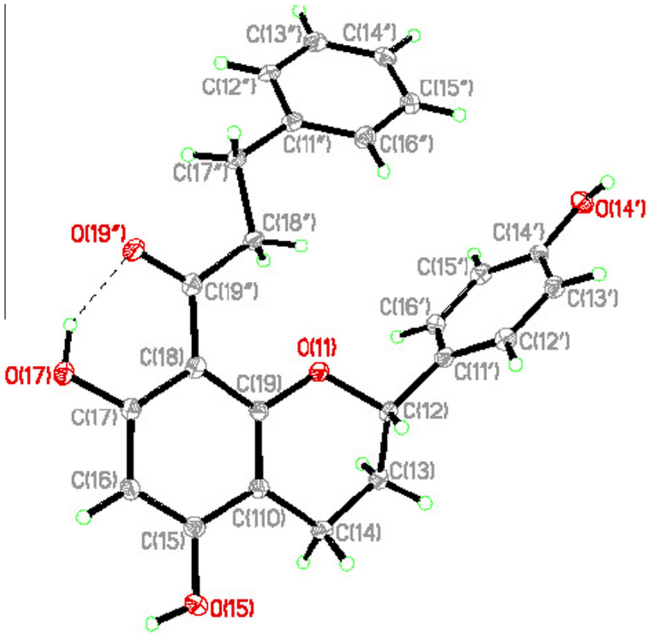

Fig. 3. Single crystal X-ray structure of **1a**.

the axial position of the half chair pyran ring was established based on the J_{2-3} coupling constant of 7.5 Hz observed, in its ^{1}H NMR spectrum. Compound (+)-**4** was assigned to having a 2*R*,3*S* absolute configuration, since its ECD spectrum was well correlated with the calculated ECD spectrum of (2*R*,3*S*)-**4**. The experimental ECD spectrum of (−)-**4** was the opposite to that of (+)-**4** and the absolute configuration of (−)-**4** was, therefore, determined to be *2S,3R*. In this case, the results obtained from ECD calculations conducted for *2R,3S*-**4** indicated that the helicity rule established for flavan-3-ols (Slade et al., 2005) was not applicable for the determination of the absolute configuration of compound **4**. The J_{2-3} coupling constant of 8.4 Hz observed in the ^{1}H NMR spectra of **5** and **6** also indicated a 2,3-trans relative configuration. The absolute configurations of (−)-**5** and (−)-**6** were established as 2*R*,3*S*, based on good agreement of the respective experimental ECD spectrum with the calculated ECD spectrum for (2*R*,3*S*)-**5** and (2*R*,2*S*)-**6** (Fig. 4). The experimental ECD spectrum of (+)-**5** and (+)-**6** showed CEs of opposite sign to those present in spectrum of (−)-**5** and (−)-**6** indicating a 2*S*,3*R* absolute configuration.

Proposed biosynthetic pathway

Recently, it was proposed that the biosynthesis of balsacones A (**10**), B (**11**) and C (**12**) proceeded by cinnamylation of dihydrochalcones **7**, **8** and **9**, respectively (Fig. 5), which were also identified in the *P. balsamifera* buds ethanolic extract (Lavoie et al., 2013). The presence of compounds **10**–**12** in the extract and the fact that compounds **1**–**6** were isolated as racemic mixtures suggested that the later might be artifacts from the extraction process which was conducted under conditions of EtOH reflux. Indeed, the presence of **1**–**6** could be the result of an intramolecular addition of the phenol function in 2′ or 4′ on the alkene of **10**, **11** or **12**. To rule out this possibility, buds were extracted in cold EtOH for a shorter period of time. The resulting extract was submitted to fractionation using reversed phase flash chromatography. The resulting fractions were analyzed using HPLC–MS–SIM selecting ions at *m/z* 301, 391, 407, 421 and 437. As shown in Fig. 6, the presence of **1**–**6** could be confirmed in fraction II. This result suggest that **1**–**6** originated rather from the buds.

A potential biosynthetic pathway for racemic mixtures **1**, **2** and **3** could consist of a non-stereospecific cyclization between C-2′-OH and C-7″ in compounds **12**, **11** and **10,** respectively (Fig. 5). Formation of racemic mixtures **5** and **6** could then be explained by a trans-hydroxylation in position 3 of the racemic mixtures **1** and **2,** respectively. Additionally, non-stereospecific intramolecular cyclization between C-4′-OH and C-7″ in compound **12** followed by a trans-hydroxylation in position 3 would explain the formation of racemic mixture **4** (Fig. 5). Recently, a pair of flavonol racemates and a flavonol racemic mixture having similar structures to compounds **1**–**6** were isolated from chinese propolis (Sha et al., 2009). The fact that they also appear as racemic mixtures in the propolis extract suggests that their biosynthesis might be related to that of compounds **1**–**6**.

*Antibacterial activity and cytotoxicity of enantiomers pairs from **1**–**6***

Antibacterial activity of pairs of enantiomers **1**–**6** was evaluated against *S. aureus* after 24 h of incubation and the results were expressed as minimal inhibitory concentration (MIC). Chloramphenicol and gentamycin were used as positive controls and showed MIC of 0.94 and 0.02 μM, respectively. Compounds (−)-**1** and (+)-**1** possess higher activity than the other pairs of enantiomers tested (**2**–**6**), with a MIC of 6.25 μM for both compounds. No difference was observed between the activity of the (+) and the (−) enantiomers for the six pairs evaluated. Compounds (−)-**4**, (+)-**4**, (−)-**5**, (+)-**5**, (−)-**6** and (+)-**6** were found active with MIC ranging from 25 to 50 μM, while compounds (−)-**2**, (+)-**2**, (−)-**3** and (+)-**3** were inactive at a concentration of 50 μM. These results suggest that an hydroxyl group at position 4 (compounds (−)-**5** and (+)-**5**) or a methoxy group at position 4″ (compounds (−)-**2** and (+)-**2**) decrease antibacterial activity. Previously reported antibacterial activity of balsacones A (**10**), B (**11**) and C (**12**) (Lavoie et al., 2013) on the same *S. aureus* strain (MIC ranging between 3.1 and 6.3) are similar to the activities obtained for compounds (−)-**1** and (+)-**1**. Finally, purified enantiomers cytotoxicity was evaluated on human skin fibroblasts WS1. Etoposide was used as a positive control (IC_{50} = 23 ± 3). All compounds were not cytotoxic at a concentration of 50 μM.

Concluding remarks

Isolation of racemic mixtures from plant extracts is rather uncommon (Finefield et al., 2012). In this work, 6 new compounds were isolated as racemic mixtures from an ethanolic extract of buds from *P. balsamifera*. Chiral HPLC allowed the separation of these mixtures to obtain 12 new flavan derivatives consisting of 6 pairs of enantiomers. Since it is rather exceptional to be able to obtain both enantiomers of closely related chiral compounds, the 12 new balsacones constitute a unique library of compounds. This library can be especially useful to study relations between chiral structures and their spectral data. ECD spectroscopy, for example, can be used to establish useful rules for the determination of the absolute configuration of the chroman ring in natural products. The library also contains compounds having toxicity towards *S. aureus* bacteria with MIC ranging between 6.25 and 50 μM. Further *in vitro* study of the antibacterial activity of the compounds of the library is in progress in the LASEVE laboratory to establish a clearer relation between the structures and absolute configuration of the isolated compounds and their antibacterial activity.

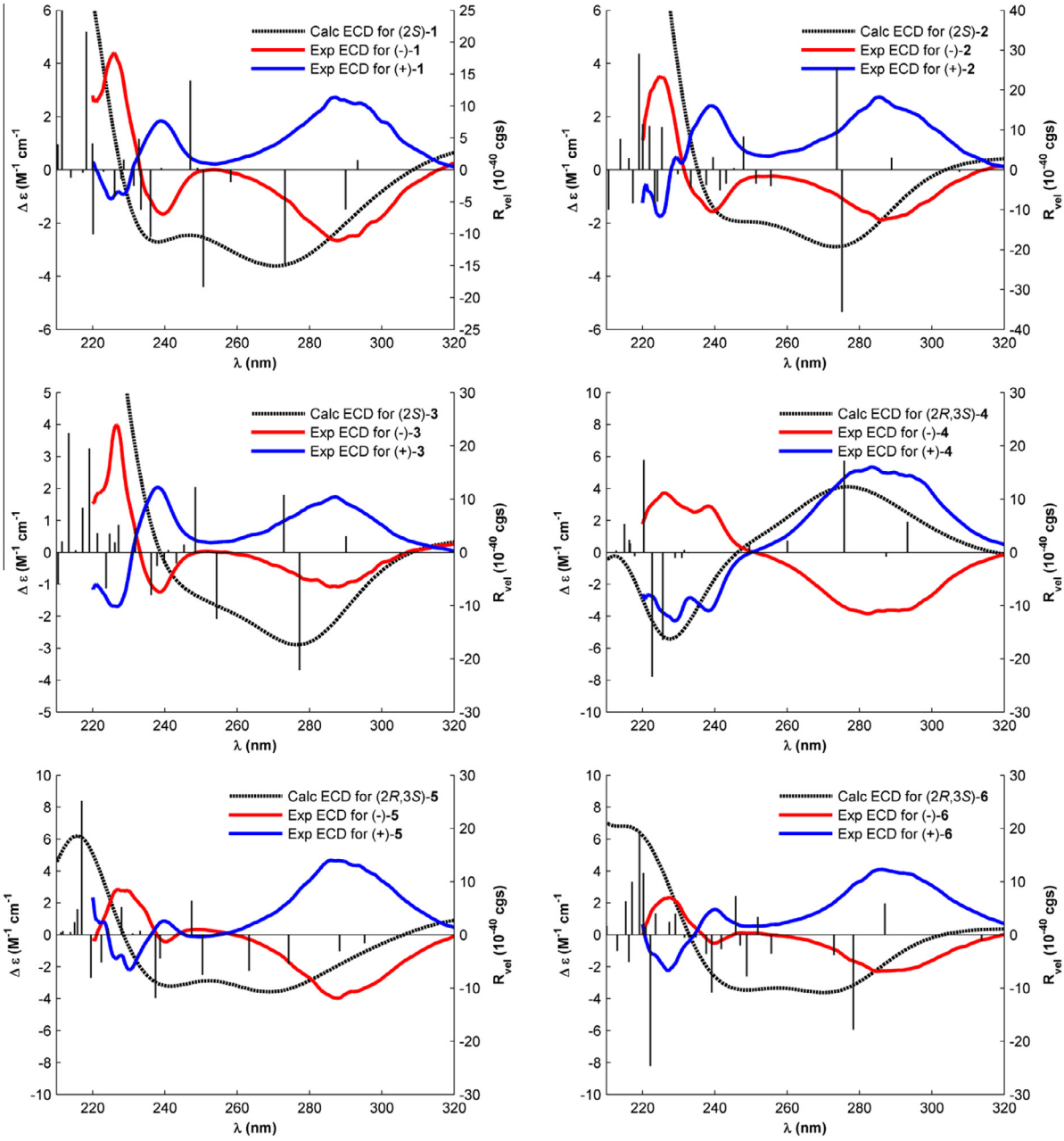

Fig. 4. Experimental ECD spectra for compounds **1**–**6** and calculated (TDDFT at the B3LYP/6-311G(2d,2p) level) EDC spectra of compounds (2S)-**1**, (2S)-**2**, (2S)-**3**, (2R,3S)-**4**, (2R,3S)-**5** and (2R,3S)-**6**.

Experimental

General

Melting points were measured with a Mettler Roledo MP70 melting point system (60–350 °C, 5 °C/min, uncorr.). Optical rotations were obtained at the sodium D line (589 nm) on a Rudolph Research Analytical Autopol IV automatic polarimeter. Absorption UV–Vis spectra were recorded using an Agilent 8453 diode-array spectrophotometer while ECD spectra were measured on a Jasco J-815 ECD spectrometer. FTIR spectra were acquired on a Perkin-Elmer SpectrumOne (neat, thin films on NaCl plates). The 1D and 2D NMR spectra (^{1}H–^{1}H COSY, NOESY, HSQC and HMBC) were obtained using an Avance 400 Bruker spectrometer (400.13 MHz for ^{1}H, 100.61 MHz for ^{13}C spectra) equipped with a 5 mm QNP probe. All spectra were acquired in acetone-d_6 and chemical shifts were reported in ppm (δ) relative to TMS. High resolution electrospray ionisation mass spectra were recorded on an Agilent Technology 6210 TOF MS system. APCI MS (positive mode) spectrum were obtained with an Agilent 1100 series HPLC equipped with an Agilent G1946 VL Mass Selective Detector in the positive mode at 70 eV. The column used for HPLC-APCI MS analysis was an Inerstil Prep ODS column (6 × 250 mm, 10 μm) at a flow rate of 1 ml/min. HPLC–MS–SIM analysis were conducted using a Zorbax Eclips XDB-C18 column (4.6 × 250 mm, 5 μm) selecting ions at *m/z* 301, 391, 407, 421 and 437 at 1 ml/min on the same instrument. Semi-preparative HPLC was carried out on an Agilent 1100 HPLC series with an Inerstil Prep ODS column (20 x 250 mm, 10 μm) at a flow rate of 10 ml/min and Chiral semi-preparative HPLC with a tris-(3,5-dimethylphenyl)carbamoyl amylose chiral coated

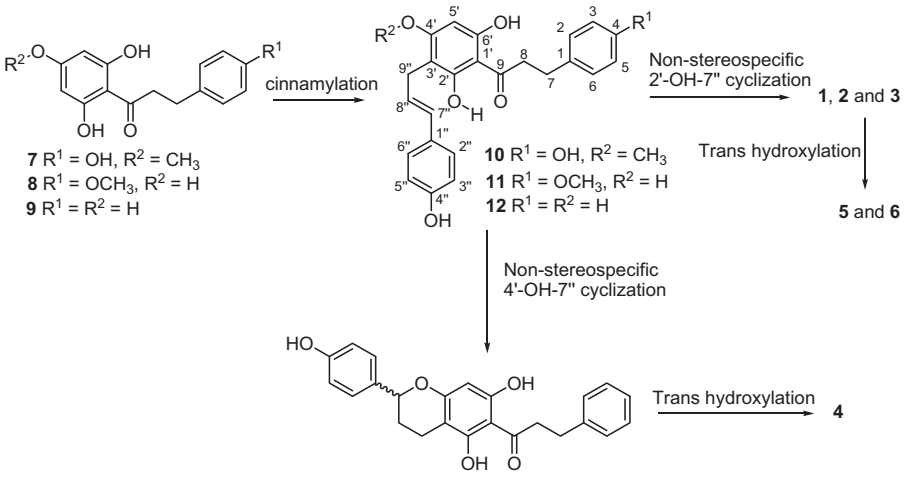

Fig. 5. Proposed biosynthetic pathway.

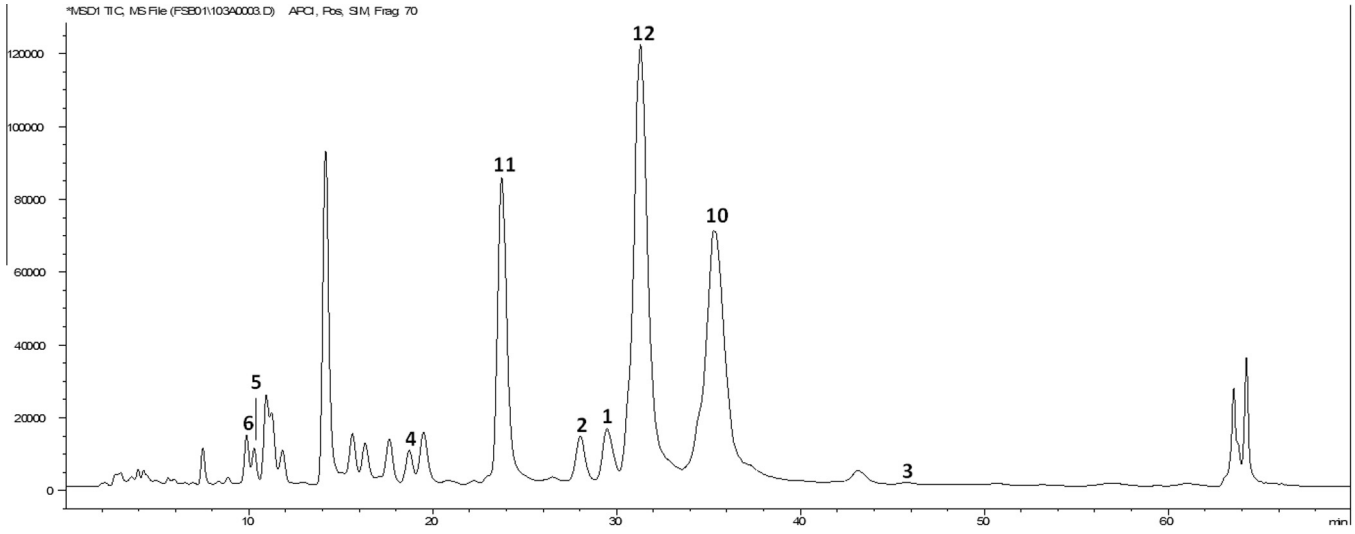

Fig. 6. HPLC–MS–SIM chromatogram trace of fraction II obtained from a cold solvent extract.

column (RegisPack™, 10 × 250 mm, 5 μm) at a flow rate of 4 ml/min. Reversed phase flash chromatography was conducted on a Biotage Flash+ system using a C18 40iM cartridge (carbon loading 17%, 135 g) from Silicycle Inc. (Ville de Québec, Québec, Canada). Reagents and analytical grade solvents were purchased from VWR International (Ville Mont-Royal, Québec, Canada) and were used as received. Ultra pure silica gel (40–63 μm) and glass TLC plates (40–63 μm with F_{254} indicator) were supplied by Silicycle Inc. (Ville de Québec, Québec, Canada).

Plant material

Buds from different trees of *P. balsamifera* were collected in March 2005 in the Chicoutimi region, Québec, Canada. The plant was authenticated by Mr. Patrick Nadeau (Université du Québec à Chicoutimi) and a voucher specimen (No. 499678) was deposited at the Louis-Marie Herbarium of Université Laval, Québec City, Québec, Canada. After collection, buds were kept frozen until extraction.

Extraction and isolation

Buds (1036 g) previously immersed in li. N_2 were coarsely ground using an electrical blender. The resulting crude powder was extracted 5 times (5 h each time) with EtOH–H_2O (95:5, V/V) 2.5 L, under conditions of reflux and the extracts were combined. After evaporation of the solvent using a rotary evaporator, the residue was suspended in MeOH and washed with hexanes. The dried MeOH residue (380.4 g) was suspended in Et_2O and extracted with H_2O. The dried Et_2O phase (355.1 g) was submitted to three successive fractionation steps: (1) silica gel CC ($CHCl_3$–MeOH, 40:1, 20:1, 10:1, 0:1); (2) silica gel CC ($CHCl_3$–MeOH, 40:1, 30:1, 20:1, 10:1, 0:1); (3) C18 flash chromatography (MeOH–H_2O, 65:35, 70:30, 72:28, 0:100). The third fractionation step afforded 5 fractions (A–E). Fraction A (19.3 g) was suspended in a $CHCl_3$–EtOAc mixture (10:1, 100 ml) and filtrated. The filtrate was recovered, dried, and the residue (5.7 g) was submitted to silica gel CC ($CHCl_3$–EtOAC, 5:1, 4:1, 3:1, 2:1, 1:1, followed by MeOH) to afford 9 subfractions (A1–A9). A1 (261.2 mg) was purified by semi-preparative HPLC (CH_3CN–H_2O, 50:50) to yield racemic mixture **1** (T_R = 33.3 min, 58.3 mg) which was purified by chiral semi-preparative HPLC (Hexane-IPA, 92:8) to afford (−)-**1** (T_R = 21.9 min, 15.9 mg) and (+)-**1** (T_R = 23.2 min, 18.5 mg). A2 (152.5 mg) was submitted to semi-preparative HPLC (CH_3CN–H_2O, 50:50) to obtain racemic mixture **2** (T_R = 31.2 min, 18.3 mg) which was purified by chiral semi-preparative HPLC (hexane-IPA, 92:8) to afford (−)-**2** (T_R = 25.9 min, 8.6 mg) and (+)-**2** (T_R = 28.7 min, 6.1 mg). A3

(119.7 mg) was applied to a semi-preparative HPLC (MeOH–H_2O, 80:20 → 100:0, 30 min) to yield racemic mixture **3** (T_R = 15.9 min, 30.0 mg) which was purified by chiral semi-preparative HPLC (hexane-IPA, 90:10) to obtain (−)-**3** (T_R = 26.7 min, 6.5 mg) and (+)-**3** (T_R = 29.1 min, 6.1 mg). A4 (545.0 mg) was subjected to two semi-preparative HPLC purification steps [(1) MeOH–H_2O, 75:25; (2) CH_3CN–H_2O, 50:50] to obtain racemic mixture **4** (T_R = 22.8 min, 15.2 mg) which was submitted to chiral semi-preparative HPLC (hexane-IPA, 85:15) to yield (−)-**4** (T_R = 32.5 min, 3.4 mg) and (+)-**4** (T_R = 40.7 min, 2.5 mg). A7 (244.9 mg) was subjected to semi-preparative HPLC (MeOH–H_2O, 60:40) to obtain racemic mixture **5** (T_R = 44.5 min, 32.0 mg) which was purified by chiral semi-preparative HPLC (hexane-IPA, 90:10) to afford (−)-**5** (T_R = 25.8 - min, 12.2 mg) and (+)-**5** (T_R = 30.0 min, 12.6 mg). Fractions A8 (90.1 mg) and A9 (118.9 mg) were both subjected to semi-preparative HPLC (CH_3CN–H_2O, 40:60) and further purified by another semi-preparative HPLC (MeOH–H_2O, 65:35) to obtain racemic mixture **6** (T_R = 25.6 min, 11.2 mg) which was further purified by chiral semi-preparative HPLC (hexane-IPA, 85:15) to yield (−)-**6** (T_R = 13.0 min, 1.5 mg) and (+)-**6** (T_R = 15.7 min, 1.2 mg).

*Detection of compounds **1**–**6** in a cold solvent extract*

Buds previously immersed in li. N_2 were coarsely ground using an electrical blender. The resulting crude powder (25.0 g) was extracted three times (30 min each time) with EtOH (150 ml) on a reciprocal shaker at room temperature. Extracts were combined and evaporated to dryness (2.3 g). Part of the dry residue (500 mg) was submitted to reversed phase flash chromatography (MeOH–H_2O, 50:50, 60:40, 70:30, 80:20, 90:10, 100:0) yielding 7 fractions (I–VII). Fraction II (97.5 mg) was submitted to HPLC–MS–SIM analysis.

Physical data of new compounds

*(−)-Balsacone D [(−)-**1**]*

Yellow powder; mp 186–188; $[\alpha]_D^{22}$ −17.4 (c 0.25, Me_2CO); ECD (c 1.3 × 10^{-3} M, MeOH): $\Delta\varepsilon_{227}$ = +4.0, $\Delta\varepsilon_{239}$ = −2.0, $\Delta\varepsilon_{288}$ = −2.6; UV (MeOH) λ_{max} (logε): 210 (4.2), 293 (4.1), 330 (3.5); IR ν_{max} 3347, 1615, 1517, 1424, 1372, 1337, 1220, 1145, 1085, 988, 956, 899, 831, 699 cm^{-1}; for ^1H and ^{13}C NMR spectroscopic data, see Tables 1 and 2; APCIMS: *m/z* 391 $[M+H]^+$ (100), 271 (60); HRESIMS: *m/z* 413.1374 $[M+Na]^+$ (calcd. for $C_{24}H_{22}O_5Na^+$, 413.1359).

Table 2
^{13}C NMR spectroscopic data of compounds **1**–**6** in acetone-d6 (100 MHz).

No.	δ_c, mult.					
	1	**2**	**3**	**4**	**5**	**6**
2	79.9, d	79.9, d	79.8, d	83.3, d	83.8, d	83.8, d
3	29.1, t	29.1, t	29.1, t	67.5, d	67.1, d	67.1, d
4	20.4, t	20.4, t	20.3, t	27.7, t	29.3, t	29.4, t
5	163.2, s	163.1, s	164.7, s	165.0, s	163.3, s	164.0, s
6	96.1, d	96.0, d	92.8, d	105.4, s	96.5, d	96.5, d
7	166.0, s	166.0, s	166.1, s	160.6, s	166.1, s	165.8, s
8	105.7, s	105.7, s	106.1, s	95.1, s	105.4, s	105.1, s
9	159.7, s	159.7, s	158.7, s	161.8, s	158.7, s	158.7, s
10	102.0, s	102.0, s	102.7, s	101.2, s	101.3, s	101.5, s
1′	132.7, s	132.7, s	132.6, s	130.6, s	130.1, s	130.3, s
2′/6′	128.9, d	129.0, d	128.8, d	129.4, d	129.9, d	130.0, d
3′/5′	116.2, d	116.2, d	116.2, d	115.9, d	116.1, d	116.1, d
4′	158.3, s	158.4, s	158.4, s	158.2, s	158.4, s	158.4, s
1″	142.3, s	134.1, s	132.7, s	142.9, s	142.2, s	134.1, s
2″/6″	129.1, d	129.9, d	129.9, d	129.3, d	129.0, d	129.9, d
3″/5″	129.0, d	114.4, d	115.8, d	129.2, d	129.0, d	114.4, d
4″	126.4, d	158.7, s	156.2, s	126.7, d	126.4, d	158.7, s
7″	31.2, t	30.3, t	30.4, t	31.4, t	31.2, t	30.6, t
8″	46.1, t	46.4, t	46.6, t	46.5, t	45.9, t	46.3, t
9″	205.2, s	205.4, s	205.8, s	205.6, s	205.2, s	205.4, s
5-O–CH_3	–	–	56.3, q	–	–	–
4″-O–CH_3	–	55.4, q	–	–	–	55.3, q

*(+)-Balsacone D [(+)-**1**]*

Yellow powder; $[\alpha]_D^{21}$ +15.5 (c 0.16, Me_2CO), ECD (c 1.3 × 10^{-3} M, MeOH): $\Delta\varepsilon_{227}$ = −1.1, $\Delta\varepsilon_{239}$ = +1.8, $\Delta\varepsilon_{288}$ = +2.4; UV, IR, ^1H, ^{13}C NMR, APCIMS and ESIMS data were the same as (−)-**1**.

*(−)-Balsacone E [(−)-**2**]*

Yellow powder; $[\alpha]_D^{22}$ −9.8 (c 0.1, Me_2CO), ECD (c 1.2 × 10^{-3} M, MeOH): $\Delta\varepsilon_{224}$ = +3.8, $\Delta\varepsilon_{239}$ = −1.6, $\Delta\varepsilon_{289}$ = −1.9; UV (MeOH) λ_{max} (logε): 206 (4.1), 292 (3.9), 330 (3.3); IR ν_{max} 3400, 1622, 1512, 1440, 1424, 1373, 1243, 1220, 1147, 1086, 1030, 989, 9 55, 897, 827, 678, 598, 569, 535 cm^{-1}; for ^1H and ^{13}C NMR spectroscopic data, see Tables 1 and 2; APCIMS: *m/z* 421 $[M+H]^+$ (100), 301 (42); HRESIMS: *m/z* 421.1656 $[M+H]^+$ (calcd. for $C_{25}H_{25}O_6^+$, 421.1646).

*(+)-Balsacone E [(+)-**2**]*

Yellow powder; $[\alpha]_D^{22}$ +13.4 (c 0.09, Me_2CO), ECD (c 1.2 × 10^{-3} M, MeOH): $\Delta\varepsilon_{224}$ = −2.6, $\Delta\varepsilon_{239}$ = +2.4, $\Delta\varepsilon_{289}$ = +2.7; UV, IR, ^1H, ^{13}C NMR, APCIMS and ESIMS data were the same as (−)-**2**.

Table 1
^1H NMR spectroscopic data of compounds **1**–**6** in acetone-d6 (400 MHz).

No.	δ_H (*J* in Hz)					
	1	**2**	**3**	**4**	**5**	**6**
2	5.07, dd (11.0, 2.0)	5.08, dd (10.7, 2.3)	5.06, dd (10.8, 2,1)	4.80, d (7.5)	4.81, d (8.4)	4.79, d (8.4)
3a	2.06, m	2.11, m	2.06, m	4.09, td (7.0, 5.5)	4.15, td (8.8, 5.9)	4.15, td (8.8, 5.8)
3b	2.19, m	2.19, m	2.19, m	–	–	–
4a	2.68, m	2.70, m	2.66, m	2.55, dd (16.1, 8.1)	2.59, dd (16.0, 9.0)	2.59, dd (16.2, 9.0)
4b	2.78, ddd (17.0, 5.9, 2.4)	2.79, m	2.72, m	2.88, dd (16.1, 5.3)	3.02, dd (16.2, 5.7)	3.03, dd, (16.2, 5.9)
6	6.02, s	6.03, s	6.10, s	–	6.05, s	6.05, s
8	–	–	–	5.97, s	–	–
2′/6′	7.35, d (8.5)	7.37, d (8.5)	7.35, d (8,6)	7.24, d (8.6)	7.34, d (8.4)	7.36, d (8.6)
3′/5′	6.85, d (8.5)	6.88, d (8.5)	6.87, d (8,6)	6.84, d (8.6)	6.85, d (8.4)	6.87, d (8.6)
2″/6″	6.91, d (7.3)	6.79, d (8.7)	6.71, d (8,6)	7.29, m	6.89, d (7.2)	6.78, d (8.6)
3″/5″	7.16, t (7.3)	6.72, d (8.7)	6.64, d (8,6)	7.29, m	7.15, t (7.2)	6.71, d (8.6)
4″	7.10, t (7.3)	–	–	7.18, m	7.09, t (7.2)	–
7″	2.84, t (8.1 Hz)	2.77, m	2.75, m	3.00, t (7.7)	2.84, t (7.9)	2.76, t (7.9)
8″	3.24, m	3.19, m	3.20, m	3.43, t (7.7)	3.22, m	3.16, m
7-OH	13.82, s	13.81, s	13.92, s	–	13.76, s	13.83, s
4″-O–CH_3	–	3.74, s	–	–	–	3.74, s
5-O–CH_3	–	–	3.89, s	–	–	–

*(−)-Balsacone F [(−)-**3**]*

Yellow powder; $[\alpha]_D^{21}$ −10.0 (c 0.09, Me_2CO), ECD (c 1.2×10^{-3} M, MeOH): $\Delta\varepsilon_{227}$ = +5.0, $\Delta\varepsilon_{239}$ = −1.3, $\Delta\varepsilon_{289}$ = −1.1; UV (MeOH) λ_{max} (log ε): 224 (4.4), 287 (4.2), 327 (3.4); IR ν_{max} 3364, 2922, 2851, 1701, 1618, 1589, 1516, 1443, 1372, 1215, 1143, 1113, 1001, 969, 849, 831, 700, 613, 596, 569, 540 cm^{-1}; For ^1H and ^{13}C NMR spectroscopic data, see Tables 1 and 2; APCIMS: *m/z* 421 $[M+H]^+$ (100), 301 (89); HRESIMS: *m/z* 443.1477 $[M+Na]^+$ (calcd. for $C_{25}H_{24}O_6Na^+$, 443.1465).

*(+)-Balsacone F [(+)-**3**]*

Yellow powder; $[\alpha]_D^{23}$ +12.1 (c 0.09, Me_2CO); ECD (c 1.2×10^{-3} M, MeOH): $\Delta\varepsilon_{227}$ = −2.0, $\Delta\varepsilon_{239}$ = +2.0, $\Delta\varepsilon_{289}$ = +1.6; UV, IR, ^1H, ^{13}C NMR, APCIMS and ESIMS data were the same as (−)-**3a**.

*(−)-Balsacone G [(−)-**4**]*

Yellow powder; $[\alpha]_D^{22}$ −43.5 (c 0.03, Me_2CO), ECD (c 1.2×10^{-3} M, MeOH): $\Delta\varepsilon_{225}$ = +3.7, $\Delta\varepsilon_{238}$ = +3.0, $\Delta\varepsilon_{290}$ = −3.8; UV (MeOH) λ_{max} (log ε): 210 (4.6), 290 (4.6), 327 (3.7); IR ν_{max} 3300, 2923, 1698, 1628, 1599, 1517, 1430, 1368, 1246, 1146, 1089, 988, 921, 832, 750, 700, 560, 522 cm^{-1}; for ^1H and ^{13}C NMR spectroscopic data, see Tables 1 and 2; APCIMS: *m/z* 407 $[M+H]^+$ (100), 271 (5); HRESIMS: *m/z* 429.1330 $[M+Na]^+$ (calcd. for $C_{24}H_{22}O_6Na^+$, 429.1309).

*(+)-Balsacone G [(+)-**4**]*

Yellow powder; $[\alpha]_D^{23}$ +66.2 (c 0.03, Me_2CO), ECD (c 1.2×10^{-3} M, MeOH): $\Delta\varepsilon_{225}$ = −3.6, $\Delta\varepsilon_{238}$ = −3.8, $\Delta\varepsilon_{290}$ = +4.9; UV, IR, ^1H, ^{13}C NMR, APCIMS and ESIMS data were the same as (−)-**4**.

*(−)-Balsacone H [(−)-**5**]*

Yellow powder; $[\alpha]_D^{25}$ −38.2 (c 0.2, Me_2CO), ECD (c 1.2×10^{-3} M, MeOH): $\Delta\varepsilon_{226}$ = +3.2, $\Delta\varepsilon_{230}$ = +2.7, $\Delta\varepsilon_{239}$ = −0.4, $\Delta\varepsilon_{287}$ = −4.0; UV (MeOH) λ_{max} (log ε): 226 (4.4), 291 (4.2), 327 (3.6); IR ν_{max} 3450, 2091, 1632, 1518, 1497, 1450, 1429, 1378, 1223, 1147, 1062 cm^{-1}; for ^1H and ^{13}C NMR spectroscopic data, see Tables 1 and 2; APCIMS: *m/z* 407 $[M+H]^+$ (100), 271 (46); HRESIMS: *m/z* 445.1055 $[M+K]^+$ (calcd. for $C_{24}H_{22}O_6K^+$, 445.1048).

*(+)-Balsacone H [(+)-**5**]*

Yellow powder; $[\alpha]_D^{25}$ +36.9 (c 0.2, Me_2CO), ECD (c 1.2×10^{-3} M, MeOH): $\Delta\varepsilon_{226}$ = −2.2, $\Delta\varepsilon_{230}$ = −2.6, $\Delta\varepsilon_{239}$ = +0.9, $\Delta\varepsilon_{287}$ = +4.7; UV, IR, ^1H, ^{13}C NMR, APCIMS and ESIMS data were the same as (−)-**5**.

*(−)-Balsacone I [(−)-**6**]*

Yellow powder; $[\alpha]_D^{25}$ −16.2 (c 0.02, Me_2CO), ECD (c 0.57×10^{-3} M, MeOH): $\Delta\varepsilon_{226}$ = +2.7, $\Delta\varepsilon_{240}$ = −0.6, $\Delta\varepsilon_{288}$ = −2.3; UV(MeOH) λ_{max} (log ε): 217 (4.4), 291 (4.3), 325 (3.8); IR ν_{max} 3337, 2924, 1614, 1512, 1425, 1373, 1223, 1177, 147, 1103, 1060, 1031, 971, 933, 829 cm^{-1}; for ^1H and ^{13}C NMR spectroscopic data, see Tables 1 and 2; APCIMS: *m/z* 437 $[M+H]^+$ (100), 301 (56); HRESIMS: *m/z* 459.1431 $[M+Na]^+$ (calcd. for $C_{25}H_{24}O_7Na^+$, 459.1414).

*(+)-Balsacone I [(+)-**6**]*

Yellow powder; $[\alpha]_D^{25}$ +35.0 (c 0.02, Me_2CO), ECD (c 0.57×10^{-3} M, MeOH): $\Delta\varepsilon_{226}$ = −2.6, $\Delta\varepsilon_{240}$ = +1.69, $\Delta\varepsilon_{288}$ = +4.1; UV, IR, ^1H, ^{13}C NMR, APCIMS data were the same as (−)-**6**; HRESIMS: *m/z* 437.1586 $[M+H]^+$ (calcd. for $C_{25}H_{25}O_7^+$, 437.1595).

*X-ray crystal structure analysis of (−)-balsacone D (−)-**1***

Diffraction intensity data were collected by a Bruker smart diffractometer equipped with an APEX II CCD detector employing graphite monochromated Cu Kα radiation (λ = 1.54178 Å) at 100 K. Crystal data were: $C_{24}H_{22}O_5$, *M* = 390.42, monoclinic, space group $P2_1$, *a* = 8.42583(14) Å, *b* = 24.2381(4) Å, *c* = 9.38693(15) Å, β = 104.9617(9)°, *V* = 1852.05(5) $Å^3$, *Z* = 4, ρ = 1.400 g/cm^3, μ(CuKα) = 0.797 mm^{-1}, total reflections 104988, independent reflections 7175 (R_{int} 0.038%), final *R* indices [$I > 2\sigma$ (*I*)] *R*1 = 0.0351, *wR*2 = 0.0943, absolute structure parameter = 0.03 (11). The structure was solved by direct methods SHELXS-97 (Sheldrick, 2008) and refined with full-matrix least-squares calculations on F^2 using SHELX-97 (Sheldrick, 2008). Crystallographic data for compound (−)-**1** were deposited at the Cambridge Crystallographic Data Center (Deposition No. CDCC 919719). Copies of these data can be obtained free of charge via www.ccdc.cam.ac.uk/conts/retrieving.html or from the Cambridge Crystallographic Data Center, 12, Union Road, Cambridge, CB2 1EZ, UK. (fax: +44 1223 336033; e-mail: deposit@ccdc.cam.ac.uk).

Conformational analysis, geometrical optimization and ECD calculation

Conformational distributions for **1**–**6** were obtained through stochastic Monte Carlo guided conformational searches at the molecular mechanics (MMFF) level of theory using the Spartan'10 V1.1.0 software package (Wavefunction, Inc., Irvine, CA, 2010). These conformers were subjected to geometry optimizations by the density functional theory (DFT) method at B3LYP/6-31G(d) level on the Gaussian 09 software (Frisch et al., 2010). Selected optimized conformers (>5% of Boltzmann distribution) were then subjected to the TDDFT calculation on Gaussian 09 for 40 excited states at B3LYP/6-311G(2d,2p) level. MeOH solvent effects were taken into account using PCM model. Excitation energy (in nm) and rotatory strength in (velocity form in 10^{40} erg-esu-cm/Gauss) were thus obtained for the different states. The ECD spectra were simulated from these data by normalization, Boltzmann averaging and overlapping Gaussian functions for each transition according to:

$$\Delta\varepsilon(E) = \frac{1}{2.297 \times 10^{-39}} \frac{1}{\sqrt{2\pi}\sigma} \sum_i^A \Delta E_i R_i e^{-[(E-\Delta E_i)/(2\sigma)]^2}$$

where σ is the width of the band at 1/e height and ΔE_i and R_i are the excitation energies and rotatory strengths for transition *i*, respectively. σ = 0.15 eV and R^{vel} have been used in this work.

Antibacterial activity

Antibacterial activity against *S. aureus* was evaluated using the microdilution method as reported previously (Banfi et al., 2003; Lavoie et al., 2013). The lowest concentration at which no growth was observed after 24 h of incubation was defined as the minimum inhibitory concentration (MIC). Gentamycin and chloramphenicol were used as positive controls.

Cytotoxicity

Cytotoxicity was evaluated against human fibroblast cell line WS1 using the resazurin reduction test reported previously (Bellila et al., 2011; O'Brien et al., 2000). Cytotoxicity was expressed as the concentration inhibiting 50% of cell growth (IC_{50}). Etoposide was used as a positive control.

Acknowledgments

This project was supported by a FQRNT fonds forestier 02 Grant, NSERC (doctoral scholarship to FS) and by Fonds de recherche nature et technologies (doctoral scholarship to FS). This research has been enabled by the use of computing resources provided by WestGrid and Compute/Calcul Canada. The authors would like to thank

F. Otis and N. Voyer from PROTEO and Université Laval for their help in recording circular dichroism spectra and C. Dusseault for its technical assistance in the evaluation of antibacterial activity and cytotoxicity.

Appendix A. Supplementary data

Supplementary data associated with this article (^{1}H, ^{13}C NMR and chiral HPLC chromatograms of racemic mixtures) can be found, in the online version, at http://dx.doi.org/10.1016/j.phytochem.2013.12.018.

References

Banfi, E., Scialino, G., Monti-Bragadin, C., 2003. Development of a microdilution method to evaluate *Mycobacterium tuberculosis* drug susceptibility. J. Antimicrob. Chemother. 52, 796–800.

Bankova, V., 2005. Recent trends and important developments in propolis research. Evid. Based Complement. Altern. Med. 2, 29–32.

Bankova, V., Popova, M., Bogdanov, S., Sabatini, A.G., 2002. Chemical composition of European propolis: expected and unexpected results. Z. Naturforsch. [C] 57, 530–533.

Bellila, A., Tremblay, C., Pichette, A., Marzouk, B., Mshvildadze, V., Lavoie, S., Legault, J., 2011. Cytotoxic activity of withanolides isolated from Tunisian *Datura metel* L. Phytochemistry 72, 2031–2036.

Chen, F., Liu, C.-J., Tschaplinski, T.J., Zhao, N., 2009. Genomics of secondary metabolism in *Populus*: interactions with biotic and abiotic environments. Crit. Rev. Plant Sci. 28, 375–392.

Christov, R., Trusheva, B., Popova, M., Bankova, V., Bertrand, M., 2006. Chemical composition of propolis from Canada, its antiradical activity and plant origin. Nat. Prod. Res. 20, 531–536.

Dickmann, D.I., 2001. An overview of the genus *Populus*. In: Dickmann, D.I., Isebrands, J.G., Eckenwalder, J.E., Richardson, J. (Eds.), Poplar Culture in North America. NRC Research Press, Ottawa, pp. 1–42.

Dudonné, S., Poupard, P., Coutière, P., Woillez, M., Richard, T., Mérillon, J.-M., Vitrac, X., 2011. Phenolic composition and antioxidant properties of poplar bud (*Populus nigra*) extract: Individual antioxidant contribution of phenolics and transcriptional effect on skin aging. J. Agric. Food Chem. 59, 4527–4536.

Eckenwalder, J.E., 1996. Systematics and evolution of Populus. In: Stettler, R.F., Bradshaw, H.D., Jr., Heilman, P.E., Hinckley, T.M. (Eds.), Biology of Populus and Its Implications for Management and Conservation. NRC Research Press, Ottawa, Canada, pp. 7–32.

Finefield, J.M., Sherman, D.H., Kreitman, M., Williams, R.M., 2012. Enantiomeric natural products: occurrence and biogenesis. Angew. Chem. Int. Ed. 51, 4802–4836.

Frisch, M.J., Trucks, G.W., Schlegel, H.B., Scuseria, G.E., Robb, M.A., Cheeseman, J.R., Scalmani, G., Barone, V., Mennucci, B., Petersson, G.A., Nakatsuji, H., Caricato, M., Li, X., Hratchian, H.P., Izmaylov, A.F., Bloino, J., Zheng, G., Sonnenberg, J.L., Hada, M., Ehara, M., Toyota, K., Fukuda, R., Hasegawa, J., Ishida, M., Nakajima, T., Honda, Y., Kitao, O., Nakai, H., Vreven, T., Montgomery Jr., J.A., Peralta, J.E., Ogliaro, F., Bearpark, M., Heyd, J.J., Brothers, E., Kudin, K.N., Staroverov, V.N., Keith, T., Kobayashi, R., Normand, J., Raghavachari, K., Rendell, A., Burant, J.C., Iyengar, S.S., Tomasi, J., Cossi, M., Rega, N., Millam, J.M., Klene, M., Knox, J.E., Cross, J.B., Bakken, V., Adamo, C., Jaramillo, J., Gomperts, R., Stratmann, R.E., Yazyev, O., Austin, A.J., Cammi, R., Pomelli, C., Ochterski, J.W., Martin, R.L., Morokuma, K., Zakrzewski, V.G., Voth, G.A., Salvador, P., Dannenberg, J.J., Dapprich, S., Daniels, A.D., Farkas, O., Foresman, J.B., Ortiz, J.V., Cioslowski, J., Fox, D.J., 2010. Gaussian 09, Revision C.01, Gaussian, Inc., Wallingford, CT.

Greenaway, W., Whatley, F.R., 1990. Resolution of complex mixtures of phenolics in poplar bud exudate by analysis of gas chromatography—mass spectrometry data. J. Chromatogr. A 519, 145–158.

Greenaway, W., May, J., Whatley, F.R., 1989. Flavonoid aglycones identified by gas chromatography–mass spectrometry in bud exudate of *Populus balsamifera*. J. Chromatogr. 472, 393–400.

Greenaway, W., English, S., Whatley, F.R., 1992a. Relationships of *Populus* × *acuminata* and *Populus* × *generosa* with their parental species examined by gas chromatography–mass spectrometry of bud exudates. Can. J. Bot. 70, 212–221.

Greenaway, W., May, J., Scaysbrook, T., Whatley, F.R., 1992b. Compositions of bud and leaf exudates of some *Populus* species compared. Z. Naturforsch. 47, 329–334.

Isidorov, V.A., Vinogorova, V.T., 2003. GC–MS analysis of compounds extracted from buds of *Populus balsamifera* and *Populus nigra*. Z. Naturforsch. [C] 58, 355–360.

Kurkin, V.A., Zapesochnaya, G.G., Braslavskii, V.B., 1990. Flavonoids of the buds of *Populus balsamifera*. Chem. Nat. Compd. 26, 224–225.

Kurtán, T., Antus, S., Pescitelli, G., 2012. Electronic CD of Benzene and other Aromatic Chromophores for Determination of Absolute Configuration. Comprehensive Chiroptical Spectroscopy. John Wiley & Sons, Inc. (pp. 73–114).

Lavoie, S., Legault, J., Simard, F., Chiasson, É., Pichette, A., 2013. New antibacterial dihydrochalcone derivatives from buds of *Populus balsamifera*. Tetrahedron Lett. 54, 1631–1633.

Mattes, B.R., Clausen, T.P., Reichardt, P.B., 1987. Volatile constituents of balsam poplar: the phenol glycoside connection. Phytochemistry 26, 1361–1366.

Moermann, D.E., 1998. Native American Ethnobotany. Timber Press, Inc..

O'Brien, J., Wilson, I., Orton, T., Pognan, F., 2000. Investigation of the alamar blue (resazurin) fluorescent dye for the assessment of mammalian cell cytotoxicity. Eur. J. Biochem. 267, 5421–5426.

Pearl, I.A., Darling, S.F., 1968a. Studies on the barks of the family *Salicaceae*—xix: continued studies on the hot water extractives of *Populus balsamifera* bark. Phytochemistry 7, 1851–1853.

Pearl, I.A., Darling, S.F., 1968b. Studies on the barks of the family *Salicaceae*—XX: variations in the hot water extractives of *Populus balsamifera* bark. Phytochemistry 7, 1855–1860.

Pelter, A., Stainton, P., Barber, M., 1965. The mass spectra of oxygen heterocycles. II. The mass spectra of some flavonoids. J. Heterocycl. Chem. 2, 262–271.

Reichardt, P.B., Bryant, J.P., Mattes, B.R., Clausen, T.P., Chapin, F.S., Meyer, M., 1990. Winter chemical defense of Alaskan balsam poplar against snowshoe hares. J. Chem. Ecol. 16, 1941–1959.

Salatino, A., Fernandes-Silva, C.C., Righi, A.A., Salatino, M.L.F., 2011. Propolis research and the chemistry of plant products. Nat. Prod. Rep. 28, 925–936.

Sentsov, M.F., Braslovskii, V.B., Kurkin, V.A., Zapesochnaya, G.G., Bakulin, V.T., Pravdivtseva, O.E., 1997. Comparative study of the component composition of buds of some *Populus* L. species with HPLC method. Rastitel'nye Resursy 33, 51–56.

Sha, N., Guan, S.-H., Lu, Z.-Q., Chen, G.-T., Huang, H.-L., Xie, F.-B., Yue, Q.-X., Liu, X., Guo, D.-A., 2009. Cytotoxic constituents of Chinese propolis. J. Nat. Prod. 72, 799–801.

Sheldrick, G.M., 2008. A short history of SHELX. Acta Crystallogr. A 64, 112–122.

Slade, D., Ferreira, D., Marais, J.P.J., 2005. Circular dichroism, a powerful tool for the assessment of absolute configuration of flavonoids. Phytochemistry 66, 2177–2215.

Tsai, C.-J., Harding, S.A., Tschaplinski, T.J., Lindroth, R.L., Yinan, Y., 2006. Genome-wide analysis of the structural genes regulating defense phenylpropanoid metabolism in *Populus*. New Phytol. 172, 47–62.

Vardar-Ünlü, G., Silici, S., Ünlü, M., 2008. Composition and in vitro antimicrobial activity of *Populus* buds and poplar-type propolis. World J. Microbiol. Biotechnol. 24, 1011–1017.